

## Electronic supplementary information for the manuscript

### Molecular structure – electrical performance relationship for OFET-based memory elements comprising unsymmetrical photochromic diarylethenes

Dolgor D. Dashitsyrenova, Andrey G. Lvov, Lyubov A. Frolova, Alexander V. Kulikov, Nadezhda N. Dremova, Valerii Z. Shirinyan, Sergey M. Aldoshin, Mikhail M. Krayushkin, and Pavel A. Troshin

#### Contents

Experimental procedures .....	3
Table S1. Spectral properties of diarylethenes <b>TO-0</b> , <b>TO-1</b> and <b>TO-2</b> before and after exposure to UV light (365 nm) in acetonitrile .....	4
Figure S1. Absorption spectra of compounds <b>TO-0</b> , <b>TO-1</b> and <b>TO-2</b> before exposure to UV light (in acetonitrile, $C = 2.7 \times 10^{-5}$ M).....	4
Figure S2. Absorption spectra of compounds <b>TO-0</b> , <b>TO-1</b> and <b>TO-2</b> after exposure to UV light (365 nm) in acetonitrile ( $C = 2.7 \times 10^{-5}$ M).....	5
Figure S3. SEM image of the OFET cross-section.....	5
Figure S4. SEM images of 1:1 (w/w) blend films comprising of diarylethene <b>TO-0</b> (a), <b>TO-1</b> (b) or <b>TO-2</b> (c) and $C_{60}$ in two different magnifications.....	6
Figure S5. Evolution of the transfer characteristics of the devices comprising <b>TO-0</b> under simultaneous exposure to a negative (a) or positive (b) applied bias voltage ( $V_p = -5$ V or $+5$ V) and violet light ( $\lambda = 405$ nm) as a function of the programming time. ....	6
Figure S6. Evolution of the transfer characteristics of the devices comprising <b>TO-1</b> under simultaneous exposure to a negative (a) or positive (b) applied bias voltage ( $V_p = -5$ V or $+5$ V) and violet light ( $\lambda = 405$ nm) as a function of the programming time. ....	6
Figure S7. Evolution of the transfer characteristics of the devices comprising <b>TO-2</b> under simultaneous exposure to a negative (a) or positive (b) applied bias voltage ( $V_p = -5$ V or $+5$ V) and violet light ( $\lambda = 405$ nm) as a function of the programming time. ....	7
Figure S8. Evolution of the transfer characteristics of the devices comprising <b>TO-0</b> under simultaneous exposure to violet light ( $\lambda = 405$ nm) and electric bias (both applied for a fixed programming time $t_p = 100$ ms) as a function of the bias voltage.....	7
Figure S9. Evolution of the transfer characteristics of the devices comprising <b>TO-1</b> under simultaneous exposure to violet light ( $\lambda = 405$ nm) and electric bias a function of the bias voltage. The programming times were fixed at 100 ms (a) and 2 s (b).....	7
Figure S10. Evolution of the transfer characteristics of the devices comprising <b>TO-2</b> under simultaneous exposure to violet light ( $\lambda = 405$ nm) and electric bias a function of the bias voltage. The programming time was fixed at 100 ms (a) and 10 ms (b).....	8
Figure S11. The absorption spectra of thin films of $C_{60}$ , <b>TO-1</b> and bilayer film <b>TO-1</b> / $C_{60}$ .....	8
Figure S12. ESR spectra of an individual $C_{60}$ film recorded at 123K in dark and under illumination with violet light (405 nm) showing no photoinduced signals.....	8

Figure S13. Proposed stabilization of the positive charge via oxidative cyclization of **TO-0** (a).  
Schematic switching mechanism for OFETs comprising **TO-0** (b).....9

## Experimental procedures

### *Materials and Instrumentation*

The devices were fabricated using a procedure described previously (L. I. Leshanskaya et al., *Adv. Optical Mater.*, 2017, 5, 1601033) with small modifications. Aluminum gate electrodes (180 nm thick) were deposited by thermal evaporation in vacuum ( $2 \times 10^{-6}$  mbar) through a shadow mask. Thin layer of  $\text{AlO}_x$  ( $\sim 10$  nm) was grown via electrochemical anodic oxidation of aluminum gate electrodes in 0.1 M citric acid (Acros Organics) at a constant potential of 35 V for 6 min. Afterwards, the photochromic layer of a diarylethene **TO-0**, **TO-1** or **TO-2** (with the thickness 60-100 nm) was formed by spin-coating 25  $\mu\text{L}$  of 10 mg/mL toluene solution atop  $\text{AlO}_x$  at 750 rpm inside a nitrogen glove box. Then the samples were transferred to the vacuum chamber, where fullerene  $\text{C}_{60}$  (32-70 nm) was deposited by thermal evaporation at the pressure of  $8 \times 10^{-6}$  mbar with the rate of 0.3–0.5  $\text{\AA}/\text{s}$  at 290-320  $^\circ\text{C}$ . Finally, silver (100 nm) was thermally evaporated through a shadow mask to form the source and drain electrodes with a channel length and width of 80  $\mu\text{m}$  and 2 mm, respectively. The layer thicknesses were confirmed by depositing the single-component films on glass in the same regime as while fabricating the device and profiling them through a scratch in a contact mode using NTEGRA PRIMA NT-MDT probe microscope.

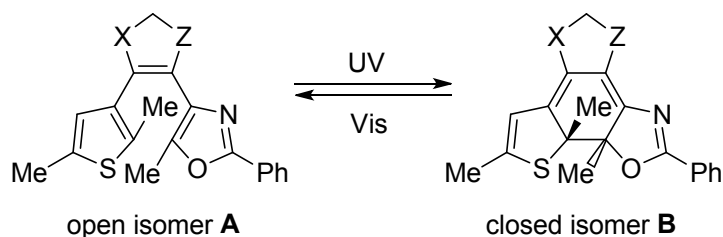
### *Measuring the electrical characteristics of OFET-based memory devices*

The procedure was essentially the same as reported previously (L. A. Frolova et al., *Chem. Commun.*, 2015, 51, 6130–6132). The electrical characterization of the devices was performed using a double-channel Keithley 2612A instrument. While programming the memory elements, an electrical bias between the source and gate electrodes of the transistor (programming voltage  $V_p$ ) and illumination provided by diode laser (405 nm,  $\sim 60 \text{ mW}\cdot\text{cm}^{-2}$ ) were applied simultaneously. The length of the single laser pulse was modulated within the range from 1 ms to 60 s using Advantest R6240A voltage current source/monitor. The transfer characteristics of the transistors and drain currents at constant gate voltage were registered after each programming step. All measurements were carried out inside a nitrogen glove box with  $<1$  ppm  $\text{O}_2$  and  $<1$  ppm  $\text{H}_2\text{O}$ .

### *Light-enhanced spin resonance (LESR) spectroscopy*

To perform light-induced electron spin resonance measurements, composite films comprised of diarylethene **TO-1**,  $\text{C}_{60}$  and [60]PCBM with a mass ratio of the components equal to 1:1:1 were deposited on the walls of ESR quartz tubes from chlorobenzene solution. [60]PCBM was added to improve the miscibility of the components and overall uniformity of the films. Similarly, reference samples of individual  $\text{C}_{60}$  or dihetarylethenes were prepared. Measurements were performed using Radiopan SE/X-2544 spectrometer in dark and under illumination with laser light  $\lambda=405$  nm at 123 K (liquid nitrogen cooling) and also in dark at room temperature (273 K).

Table S1. Spectral properties of diarylethenes **TO-0**, **TO-1** and **TO-2** before and after exposure to UV light (365 nm) in acetonitrile



Diarylethene	Structure	$\lambda_{\max}^A$ , nm ( $\epsilon$ , $M^{-1}\cdot\text{cm}^{-1}$ ) <sup>a</sup>	$\lambda_{\max}^B$ , nm ( $\epsilon$ , $M^{-1}\cdot\text{cm}^{-1}$ )
<b>TO-0</b>		290 (16500)	452 (8900)
<b>TO-1</b>		298 (26000)	523 (7600)
<b>TO-2</b>		284 (24300)	549 (6000)

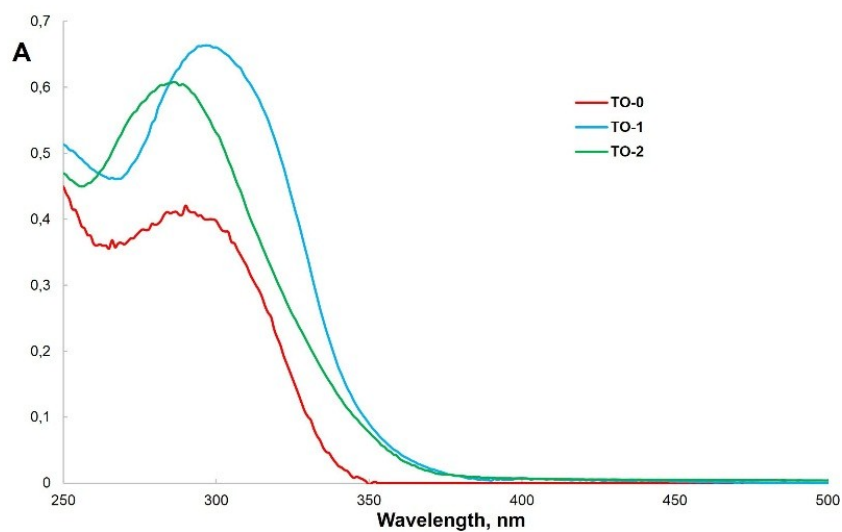


Figure S1. Absorption spectra of compounds **TO-0**, **TO-1** and **TO-2** before exposure to UV light (in acetonitrile,  $C = 2.7 \times 10^{-5}$  M).

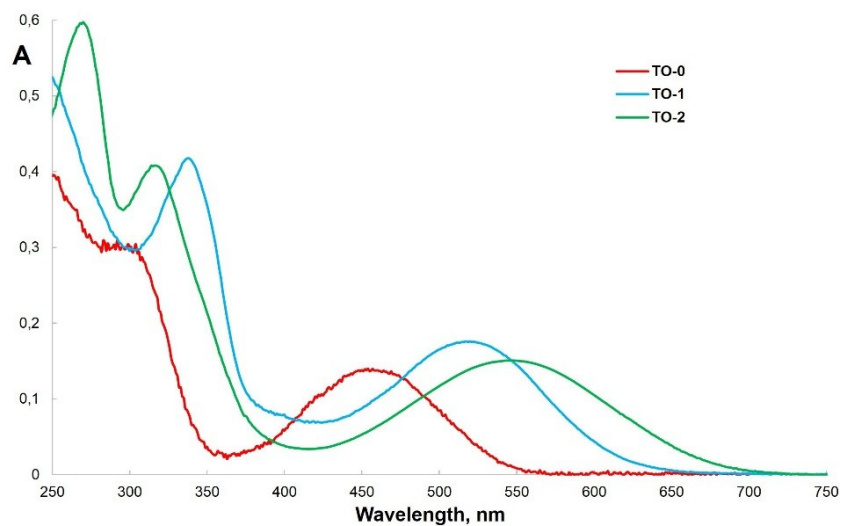


Figure S2. Absorption spectra of compounds **TO-0**, **TO-1** and **TO-2** after exposure to UV light (365 nm) in acetonitrile ( $C = 2.7 \times 10^{-5} \text{ M}$ ).

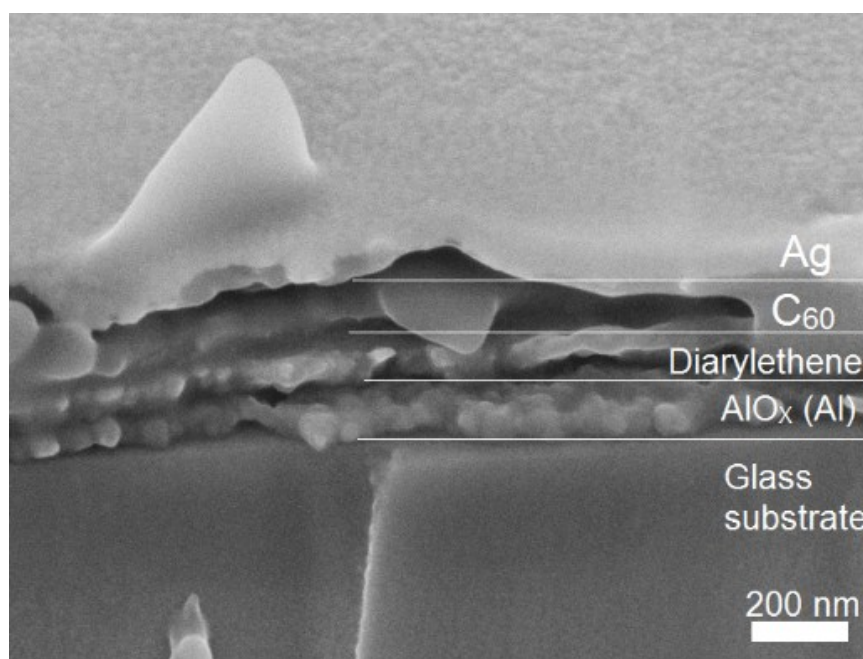


Figure S3. SEM image of the OFET cross-section.

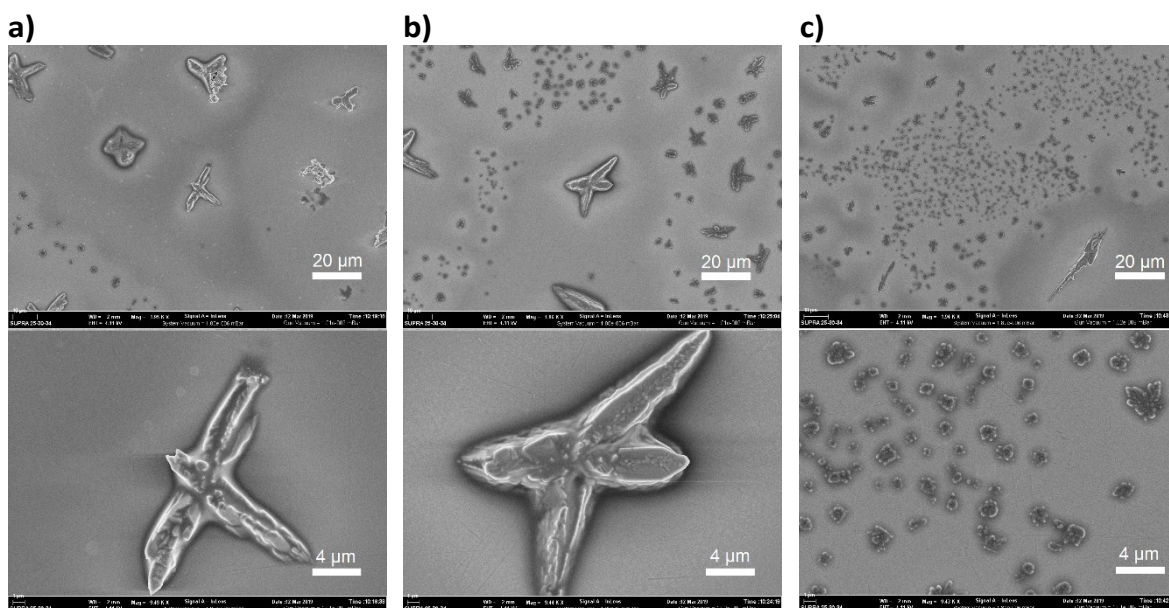


Figure S4. SEM images of 1:1 (w/w) blend films comprising of diarylethene **TO-0** (a), **TO-1** (b) or **TO-2** (c) and  $C_{60}$  in two different magnifications.

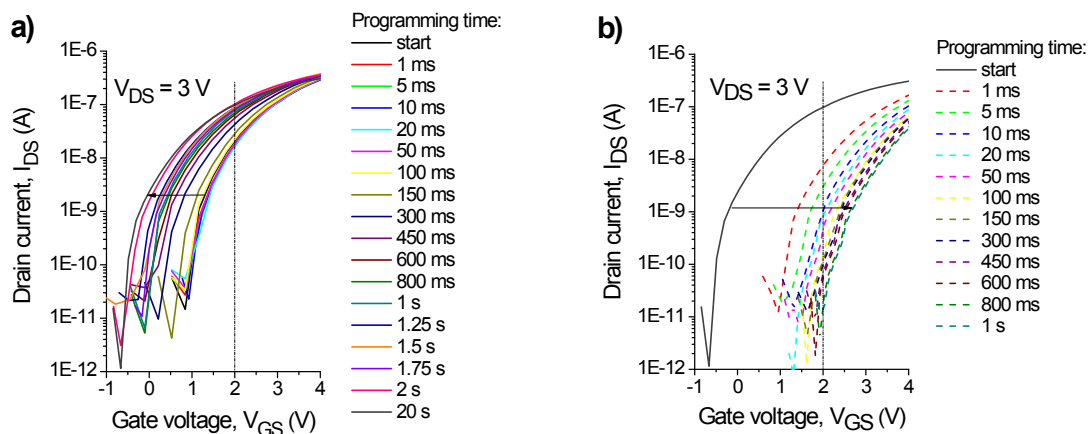


Figure S5. Evolution of the transfer characteristics of the devices comprising **TO-0** under simultaneous exposure to a negative (a) or positive (b) applied bias voltage ( $V_p = -5$  V or  $+5$  V) and violet light ( $\lambda = 405$  nm) as a function of the programming time.

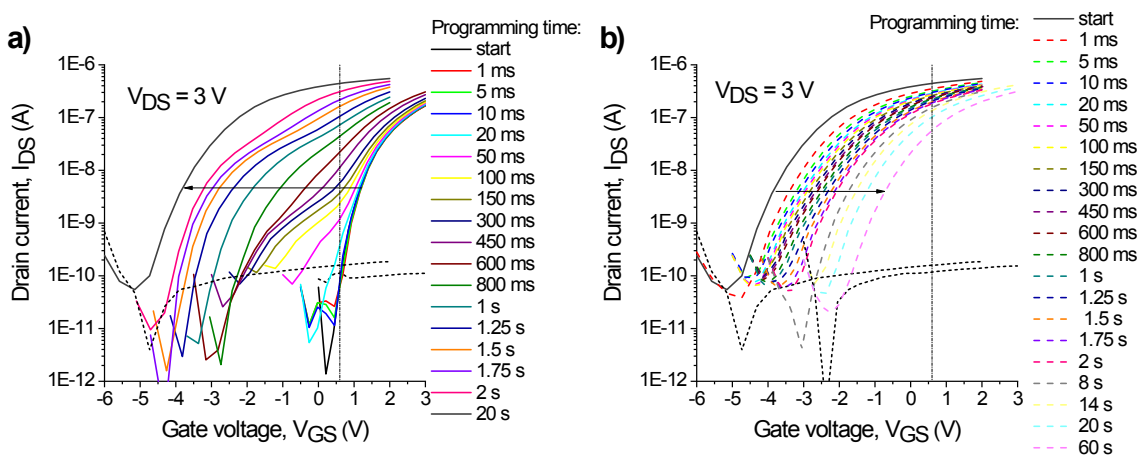


Figure S6. Evolution of the transfer characteristics of the devices comprising **TO-1** under simultaneous exposure to a negative (a) or positive (b) applied bias voltage ( $V_p = -5$  V or  $+5$  V) and violet light ( $\lambda = 405$  nm) as a function of the programming time.

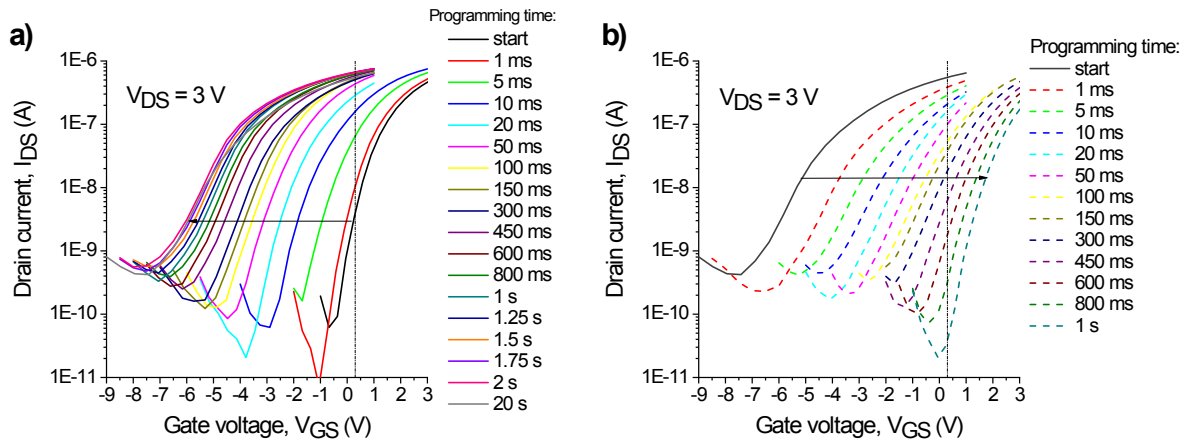


Figure S7. Evolution of the transfer characteristics of the devices comprising **TO-2** under simultaneous exposure to a negative (a) or positive (b) applied bias voltage ( $V_p = -5$  V or  $+5$  V) and violet light ( $\lambda = 405$  nm) as a function of the programming time.

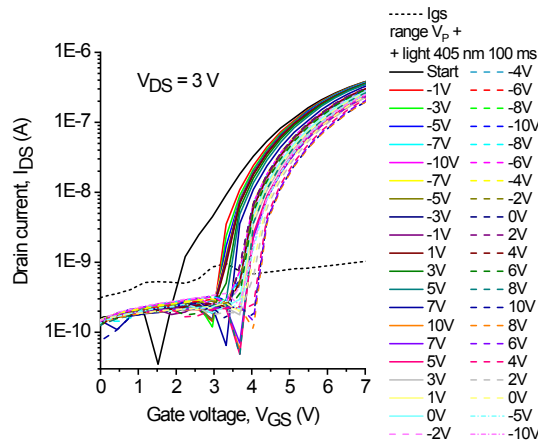


Figure S8. Evolution of the transfer characteristics of the devices comprising **TO-0** under simultaneous exposure to violet light ( $\lambda = 405$  nm) and electric bias (both applied for a fixed programming time  $t_p = 100$  ms) as a function of the bias voltage.

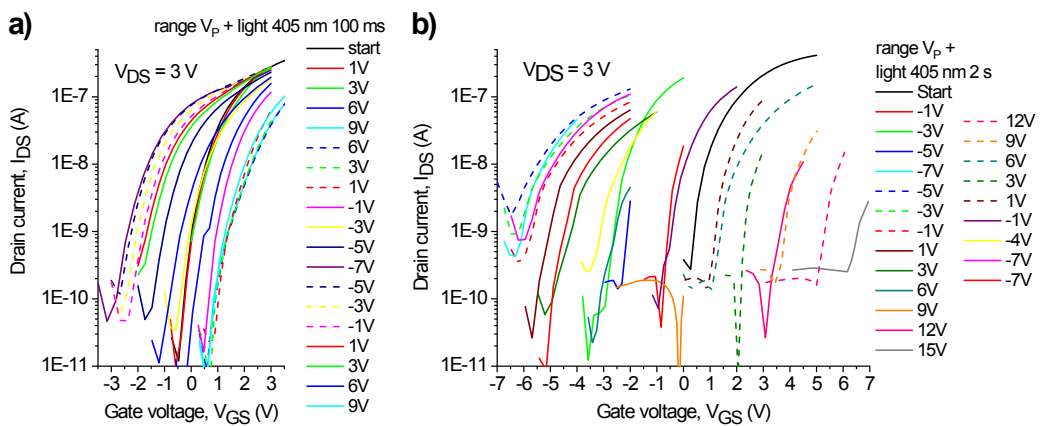


Figure S9. Evolution of the transfer characteristics of the devices comprising **TO-1** under simultaneous exposure to violet light ( $\lambda = 405$  nm) and electric bias as a function of the bias voltage. The programming times were fixed at 100 ms (a) and 2 s (b).

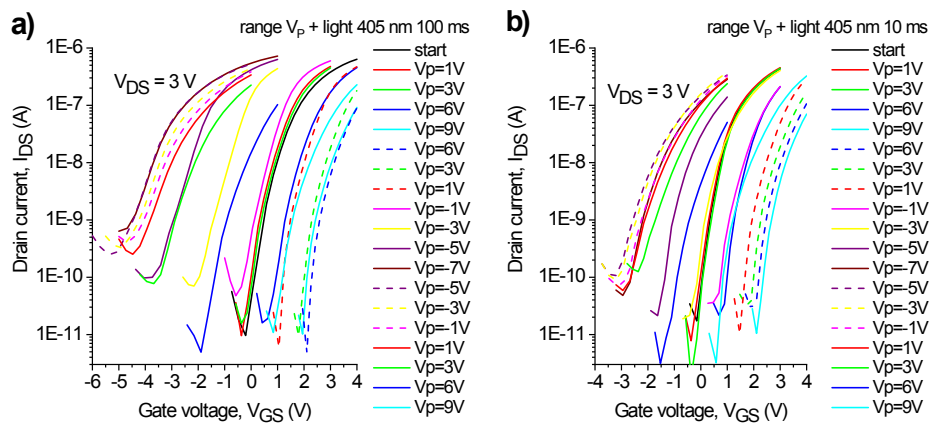


Figure S10. Evolution of the transfer characteristics of the devices comprising **TO-2** under simultaneous exposure to violet light ( $\lambda = 405 \text{ nm}$ ) and electric bias a function of the bias voltage. The programming time was fixed at 100 ms (a) and 10 ms (b).

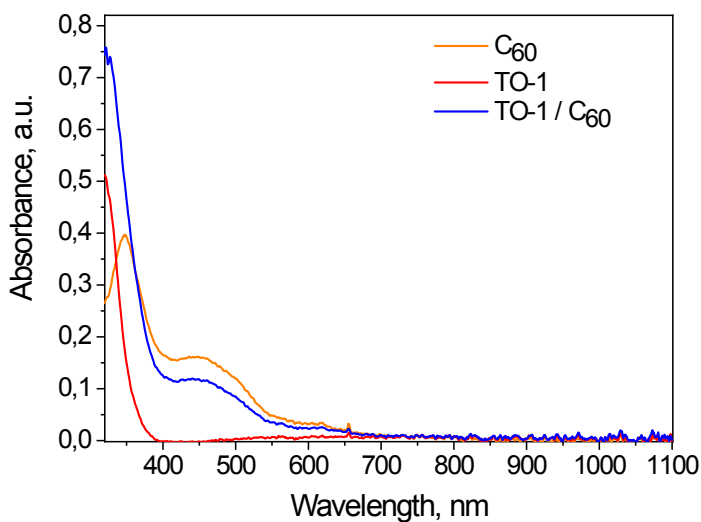


Figure S11. The absorption spectra of thin films of  $C_{60}$ , **TO-1** and bilayer film **TO-1/C<sub>60</sub>**.

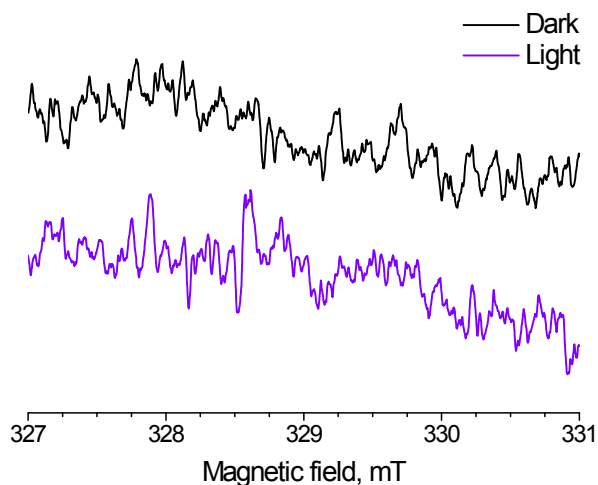


Figure S12. ESR spectra of an individual  $C_{60}$  film recorded at 123K in dark and under illumination with violet light (405 nm) showing no photoinduced signals.

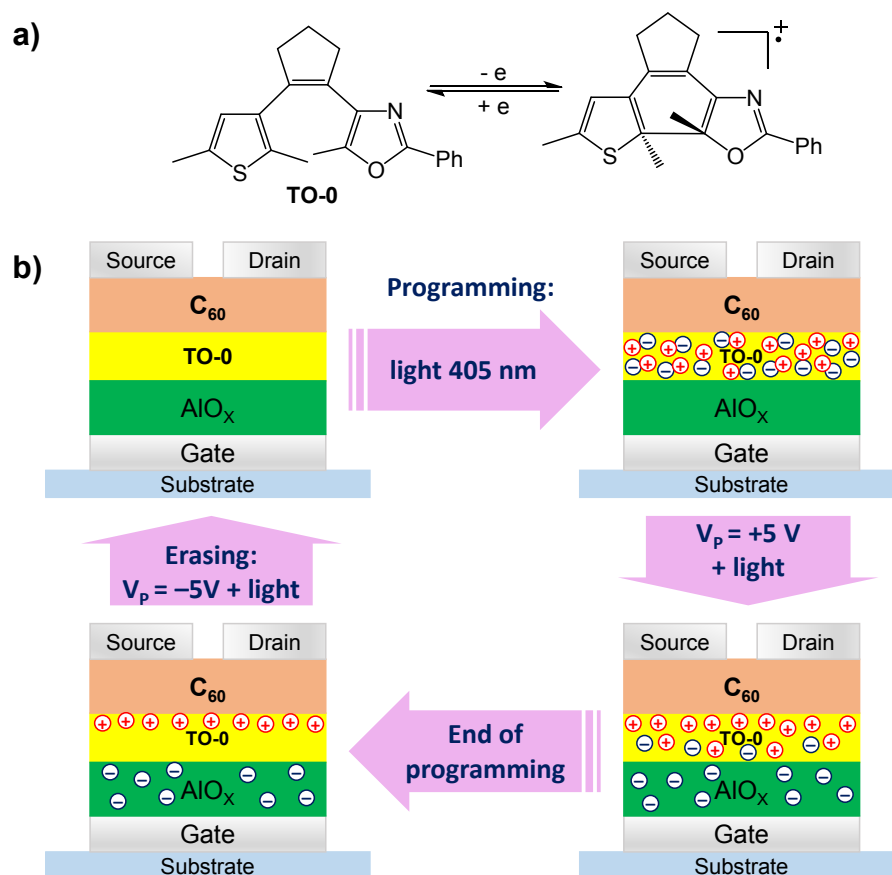


Figure S13. Proposed stabilization of the positive charge via oxidative cyclization of **TO-0** (a). Schematic switching mechanism for OFETs comprising **TO-0** (b).